Inducing formation of a corrugated, white-light emitting 2D lead-bromide perovskite via subtle changes in templating cation

Journal Name

Inducing formation of a corrugated, white-light emitting 2D lead-bromide perovskite via subtle changes in templating cation

Benny Febriansyah,[a,b,c] David Giovanni,[d] Ramesh Sankaran,[c,d] Teck Ming Koh,[b] Yongxin Li,[a] Tze Chien Sum,[d] Nripan Mathews,[b,e] and Jason England[a*]

Of a series of new 2D lead-bromide perovskites, templated by closely related dications 1–5, a corrugated (110)-oriented structure was attained only in one, 1[PbBr₄]. The others display (100) structures. Upon excitation by UV-light, 1[PbBr₄] exhibits intrinsic white-light emission that is "colder" than previously reported for this class of compounds.

Lighting accounts for one-fifth of global electricity consumption.[1] Owing to their low power consumption and high reliability, white light-emitting diodes (WLEDs) are ubiquitously used for this purpose.[2] Two-dimensional (2D) hybrid Pb-Br perovskites displaying broadband white-light emission are a particularly promising class of materials for WLED applications.[3,4] This is because they are able to function as single-source down-converting white-light-emitting phosphors that display good colour rendition and comparatively stable emission colours.[5] Additionally, these materials can be evenly deposited from solution over large surface areas, without the need of additives, making them attractive in terms of cost and ease of fabrication.[6,7]

Mechanistically, it has been proposed that broadband photoluminescence (PL) exhibited by 2D lead-bromide perovskites originates from excited electron-hole pairs stabilized by strong coupling to the easily deformable inorganic

lattice (i.e. self-trapped excitons; STEs).[8-10] As the white-light emission comes from a single-phase bulk material and its structure is highly dependent upon the cation incorporated, it should be possible to engineer the PL properties of 2D lead-bromide perovskites at a molecular level.[11] However, although desirable, relatively few compounds have been reported to exhibit such broadband PL.[7,12-19]
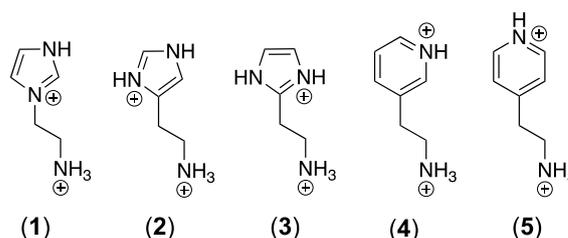

Fig. 1 The organic dications used in this study.

Whereas (100)-oriented 2D perovskites consist of flat inorganic sheets, their (110)-oriented congeners have corrugated layers. The aforementioned orientations refer to the different crystallographic planes along which the nominal parent 3D inorganic lattice has been sliced. The inherently more distorted nature of the corrugated structure would be expected to result in stronger exciton-phonon coupling and, thereby, manifest in broadband photoluminescence (PL). Indeed, we are aware of only seven examples of lead-bromide hybrid perovskites possessing (110)-oriented inorganic architecture and all of them have been reported to exhibit broadband white-light emission.[12-17,20] By comparison, only a handful of (100)-oriented structures (out of the more than 50 examples reported in the Cambridge Structural Database) feature this property.[7,9,11,17,18] Thus, any work that contributes to our understanding of the molecular design criteria required for successful formation of (110)-oriented structures, which would enable rapid expansion of this library of compounds, is of significant value.

[a]Division of Chemistry and Biological Chemistry, School of Physical and Mathematical Sciences, Nanyang Technological University, 21 Nanyang Link, Singapore 637371, Singapore.

[b]Energy Research Institute at Nanyang Technological University (ERI@N), Research Techno Plaza, X-Frontier Block Level 5, 50 Nanyang Drive, Singapore 637553, Singapore.

[c]Interdisciplinary Graduate School (IGS), 50 Nanyang Avenue, Singapore 639798 Singapore.

[d]Division of Physics and Applied Physics, School of Physical and Mathematical Sciences, Nanyang Technological University, 21 Nanyang Link, Singapore 637371, Singapore.

[e]School of Materials Science and Engineering, Nanyang Technological University, 50 Nanyang Avenue, Singapore 639798, Singapore
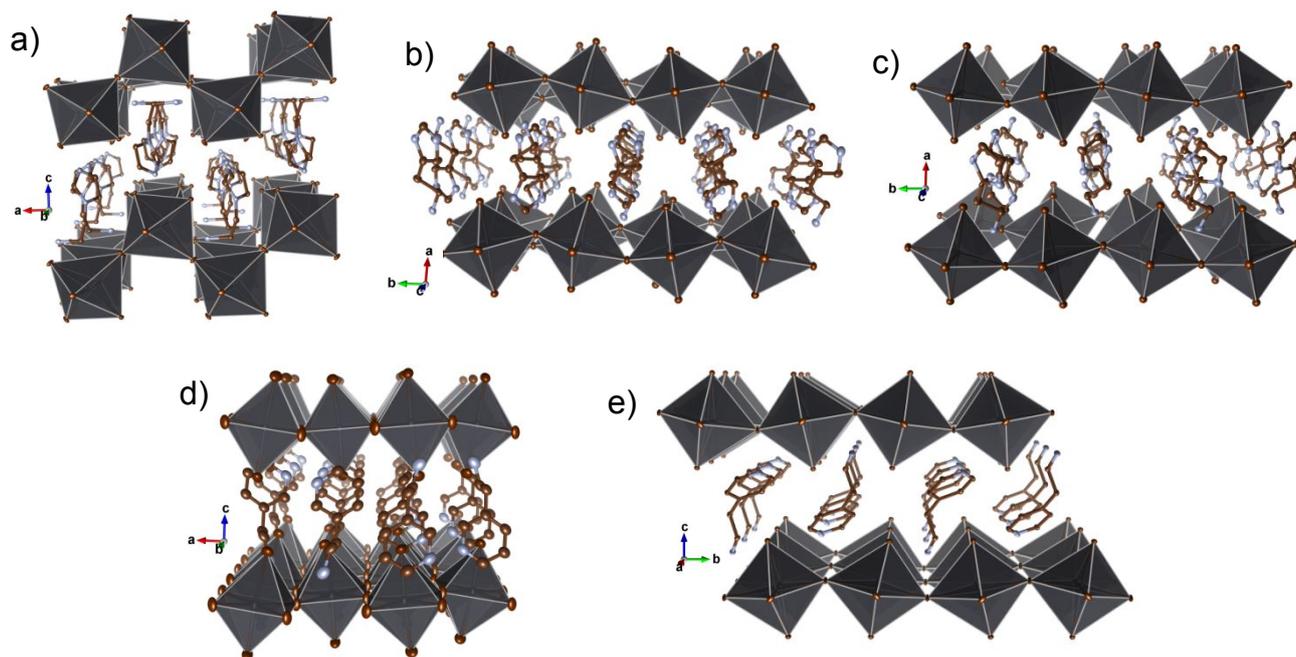
[*]E-mail: Jengland@ntu.edu.sg.

Fig. 2 Single crystal X-ray structures of the 2D perovskites a) **1**[PbBr$_4$], b) **2**[PbBr$_4$], c) **3**[PbBr$_4$], d) **4**[PbBr$_4$] and e) **5**[PbBr$_4$]. Black, maroon, brown and blue spheres represent Pb, Br, C and N atoms, respectively. H atoms are omitted for clarity. Ellipsoids are shown at 50% probability. (Larger and more detailed depictions can be found in the Supporting Information, **Figs. S2 – S10**.)

In previous work, we have shown that organic cations containing cyclic ammonium ions bearing various substituents template lead-halide perovskites displaying unusual, often highly distorted, structures.[21, 22] Such a molecular design is modular and highly flexible. Thus, a homologous series of organic cations can be readily synthesized and their impact upon the structure of the inorganic lattice can be systematically investigated. In this article, a family of dications composed of imidazolium or pyridinium cores substituted at various positions by a 2-ethylammonium chain (**Fig. 1**) have been employed in preparation of new 2D lead-bromide perovskites.

Dication **1** was previously reported (by us) to template formation of the first example of a corner-sharing "3 × 3" (110) Pb-I 2D perovskite, **1**[PbI$_4$].[22] Replacement of iodide by the smaller bromide anion, to give **1**[PbBr$_4$], leads to a 2D material that adopts "2 × 2" corrugation (**Fig. 2a**). (Crystallographic refinement data, plus selected bond lengths and angles are tabulated in the Supporting Information.) The level of corrugation, "n × n", refers to the number (n) of contiguous Pb octahedra comprising each ridge/groove. Compound **1**[PbBr$_4$] is only the seventh example of a 2D bromoplumbate framework demonstrated to possess 2 × 2 corrugation. After Lin and co-workers published two structures of this type in 2006 and 2008,[12, 13] it took more than 5 years before Karunadasa's group reported a further two.[14, 15] Recently, Kanatizidis and co-workers also reported two new compounds.[17, 20]

Intriguingly, the 2D perovskites **2**[PbBr$_4$] and **3**[PbBr$_4$], which are templated by dications that are stuctural isomers of **1** (**Fig. 1**), display more common (100)-oriented structures (**Figs. 2b-c**).

The most obvious difference between the aforementioned dications is that the endocyclic N-atoms of the imidazolium rings in **2** and **3** all bear protons (i.e., are NH+ functional groups), whereas that is true for only one of the two endocyclic N-atoms in **1**. In the latter, the other is alkylated. The greater steric bulk of this alkylated endocyclic N-atom inhibits interaction with the bromide ions of the inorganic layers and manifests in a significantly elongated N···Br interaction distance of 3.736 Å (Larger and more detailed depictions of the intermolecular hydrogen bonding interactions between the organic dications and inorganic lattices, including distances, are provided in **Figs. S1 – S10**). For reference, the longest endocyclic N···Br distances in **2**[PbBr$_4$] and **3**[PbBr$_4$] are 3.392 Å and 3.320 Å, respectively (see **Figs. S3-S6** for more details). Furthermore, the N···Br coulombic interaction of the alkylated endocyclic N-atom of **1** is perpendicular to the plane of the imidazolium ring. (Interactions with the endocyclic NH+ functional groups in **1 – 3** are exclusively in the plane of the ring.) The aforementioned factors strongly disfavour penetration of the imidazolium rings of **1** into the cuboctahedral cavities of (100)-oriented 2D inorganic layers, which are comprised of four nearest neighbour, axial, terminally-bound bromide ions. In this scenario, maximization of Coulombic interactions can be accommodated by corrugation of the 2D inorganic lattice.

In the hope of reproducing the H-bond configuration of **1**, required for formation of a corrugated structure, we turned to the pyridinium-containing dications **4** and **5**. Unfortunately, the resulting perovskites **4**[PbBr$_4$] and **5**[PbBr$_4$] still exhibit flat, (100)-oriented, bromoplumbate sheets (**Figs. 2d-e**). Although it
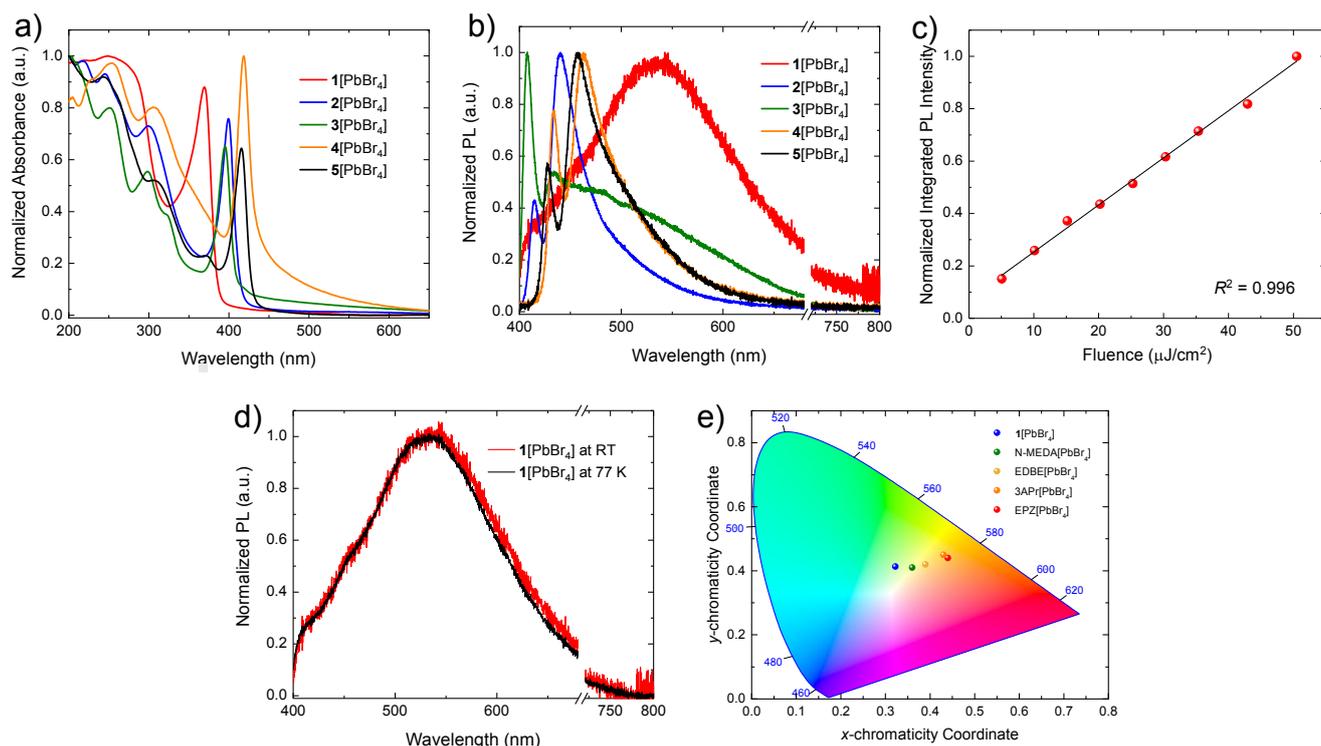
Fig. 3 Room temperature (RT) a) UV-vis absorption and b) photoluminescence (PL) spectra of **1**[PbBr$_4$] − **5**[PbBr$_4$]. c) Plot and linear fit of the dependence of PL intensity upon laser fluence for **1**[PbBr$_4$], measured at 293 K, in the range 5 - 50 µJ/cm^2. d) PL spectrum of **1**[PbBr$_4$] at RT (red line) and 77 K (black line). e) Chromaticity coordinates for the PL emission of **1**[PbBr$_4$], compared with values for previously reported 2 × 2 (110) 2D perovskites.

is possible that the larger ring size of pyridinium (relative to imidazolium) rings is a contributing factor, we believe the primary reason for this observation is the absence of an additional coulombic interaction perpendicular to plane of the heterocyclic ring (see **Figs. S7 − S10** for more detailed depictions). As such, all of the ammonium N-atoms can intrude into the cuboctahedral cavities of the (100)- oriented 2D layers and there is no driving force for corrugation of the structure.

The degree of distortion *within* the [PbBr$_6$]$^{4-}$ octahedra (i.e., intra-octahedral), which comprise the inorganic layers, was assessed for the compounds reported herein using the octahedral bond length distortion parameter Δ_{oct}.[16, 23, 24] The equation used to calculate this, and some explanation of it, is provided in the SI. Larger values correspond to greater deviation from ideal octahedral symmetry. From the average Δ_{oct} values calculated for each structure, listed in **Table S1**, it is clear that the degree of distortion experienced by the [PbBr$_6$]$^{4-}$ octahedra is the largest for **1**[PbBr$_4$] (Δ_{oct} = 22.93 × 10^{-4}). This is mainly due to its corrugated structure. Based upon literature precedent,[16] one would expect this compound to be a good candidate for broadband white-light emission.

More detailed comparison of intra-octahedral distortion of the structure of **1**[PbBr$_4$] with that of published 2 × 2 (110) 2D perovskites can be obtained using the additional parameters octahedral elongation (λ_{oct}) and octahedral angle variance (σ^2_{oct}). These two parameters quantify the deviation from O_h symmetry originating from Pb−Br bond lengths (d) and Br−Pb−Br angles (α), *via* changes in edge length (Br−Br distances) and O_h volume (V) relative to an ideal structure (see SI).[23, 24] Interestingly, while the Δ_{oct} values for all of the corrugated Pb-Br perovskites are of a similar magnitude, the λ_{oct} and σ^2_{oct} are much larger in **1**[PbBr$_4$] (**Table S2**). This can be attributed to the asymmetric nature of dicationic **1**. More specifically, it contains multiple centres of positive charge that differ significantly in terms of their steric profiles (i.e., endocyclic NH and alkylated N atoms, plus an exocyclic primary ammonium cation). As a result, the lead-bromide octahedra are presented with an inherently asymmetric charge environment.

Physically, **1**[PbBr$_4$] − **5**[PbBr$_4$] appear colourless and the UV-vis absorption spectra of these materials confirm their high bandgap natures (**Fig. 3a**). Their features are similar to those of other 2D lead−halide perovskites, in as much as the dielectric mismatch between organic and inorganic layers leads to strongly bound excitons, which results in sharp excitonic absorption bands in the region 370 − 420 nm.[3-5] Significant bathochromic shifts of this feature are observed in **4**[PbBr$_4$] and **5**[PbBr$_4$] relative to **1**[PbBr$_4$]. This is due to both the (100) structure of the former compounds and the closer approach of their Pb-(µ-Br)-Pb bond angles to ideal values (180°), which stabilizes the conduction band and, consequently, narrows their band gaps.[22, 25, 26] The remaining absorption bands, that appear

at higher energy (*ca.* 350 nm and below), in the spectra of **1**[PbBr$_4$] − **5**[PbBr$_4$] can be attributed to combinations of charge transfer transitions within and between the inorganic and organic layers and higher order exciton transition energy levels.[25]

Upon excitation with 350 nm UV light, **1**[PbBr$_4$] − **5**[PbBr$_4$] all exhibit PL emission in the visible region comprised of a narrow band and a lower energy, broad feature (**Fig. 3b**). The maxima of the former are located at similar energies ranging from 408 − 434 nm, close to their excitonic transitions. Thus, it can be assumed that the narrow emissions originate from direct relaxation of free excitons.[5, 11] As with other non-corrugated 2D Pb-Br perovskites,[7, 16] the broad emission bands in **2**[PbBr$_4$] − **5**[PbBr$_4$] are red-shifted by only ca. 25 - 30 nm relative to their respective exciton bands. In contrast, a dramatic shift of *ca.* 124 nm and extensive broadening of the low energy band is observed for **1**[PbBr$_4$]. This is consistent with expectations based upon the large intra-octahedral distortions observed for this compound (**Tables S1 and S2**) and can, in particular, be attributed to its (110)-oriented inorganic framework.

Several studies have concluded that such broadband white-light emission occurs intrinsically and it is ascribed to the self-trapped excitons formed in the disordered crystal lattice.[8-10] This type of mechanism has also been invoked for hybrid lead-halide systems of lower dimensionality, including those possessing one- and zero-dimensional inorganic lattices.[27-29] Our experimental observations concur and, therefore, the mechanism of PL in our systems is not discussed in any depth herein. For instance, power-dependent PL measurements were performed for **1**[PbBr$_4$], at 293 K, and it was observed that the PL intensity increases linearly with excitation fluence from 5 to 50 μ J/cm^2, with no signs of PL saturation (**Fig. 3c**). These observations are consistent with an intrinsic, excitonic origin for the broadband PL. In addition, no change in emission band shape is seen throughout the course of the experiment (see **Fig. S11** for evolution of the PL with excitation intensity). This indicates there is no change in the emissive defect sites accessed at different fluences. Note that **1**[PbBr$_4$] also displays similar PL features at temperatures ranging from room temperature (RT) to 77 K (**Figs. 3d and S12**). Time-resolved PL was, additionally, conducted (**Fig. S13**) and it was found that the effective PL lifetime of **1**[PbBr$_4$] is relatively short at room temperature (ca. 1.4 ns), but moderately increases upon lowering the temperature (to ca. 3.3 ns at 77 K). All of this data is consistent with previous reports of formation of self-trapped excitons in this class of materials.

RT emission of **1**[PbBr$_4$] spans across the entire visible region, is heavily Stokes-shifted (by ca. 1.05 eV), and features a large full width at half maximum (FWHM) of *ca.* 810 meV. The CIE chromaticity coordinate of its emission is shown in **Fig. S14**, along with those of the other compounds reported herein. While the emissions of **2**[PbBr$_4$] − **5**[PbBr$_4$] are located in the deep blue region, as reflected by CIE coordinates (*x*, *y*) of (0.18, 0.14), (0.25, 0.29), (0.19, 0.22) and (0.19, 0.22), respectively,

that of **1**[PbBr$_4$] is shifted much closer to the central white region. Its CIE coordinates of (0.32, 0.41) correspond to a correlated colour temperature (CCT) of 5824 K and colour rendering index (CRI) of 73. In contrast, the 2 × 2 corrugated compounds (N-MEDA)PbBr$_4$, (EDBE)PbBr$_4$, (3APr)PbBr$_4$, and (EPZ)PbBr$_4$ all possess CCTs below 5000K (4669, 3990, 3456 and 3324 K, respectively).[14, 15, 17, 20] Such values correspond to "warm" white-light emission, whereas the more blue-shifted, intense emission band in **1**[PbBr$_4$] makes it more suitable for "cold" white-light LEDs (**Fig. 3e**).

In conclusion, we report a rare 2 × 2 (110) 2D perovskite that is templated by the dication 1-(2-ammonioethyl)-1*H*-imidazol-3-ium (**1**). Its corrugated 2D bromoplumbate layers exhibit a high degree of [PbBr$_6$]$^{4-}$ intra-octahedral distortion, which manifests in broadband white-light emission, associated with large Stokes-shift and FWHM values. Furthermore, we demonstrated that access to the desired (110)-oriented structure, rather than the (100)-oriented alternative, is a consequence of the organic cation possessing a subtle balance of structural properties. In our case, inclusion of a Coloumbic interaction perpendicular to the plane of the heterocyclic ring via alkylation of an endocyclic *N*-atom. As such, this work adds to the short list of known corrugated 2D lead-halide perovskites, and provides molecular engineering insight that may contribute to the design of better performing materials in the future.

Notes

The authors declare no competing financial interest. CIF data for associated crystal structures have been deposited in the Cambridge Crystallographic Data Centre under deposition numbers CCDC 1915482-1915486.

References

1. Y. Sun, N. C. Giebink, H. Kanno, B. Ma, M. E. Thompson and S. R. Forrest, *Nature*, 2006, **440**, 908–912.
2. Z. Xia and Q. Liu, *Prog. Mater. Sci.*, 2016, **84**, 59–117.
3. B. Saparov and D. B. Mitzi, *Chem. Rev.*, 2016, **116**, 4558–4596.
4. Z. Cheng and J. Lin, *CrystEngComm*, 2010, **12**.
5. M. D. Smith and H. I. Karunadasa, *Acc. Chem. Res.*, 2018, **51**, 619–627.

6.   S. Wang, Y. Yao, J. Kong, S. Zhao, Z. Sun, Z. Wu, L. Li and J. Luo, *Chem. Commun.*, 2018, **54**, 4053–4056.

7.   H. Hu, S. A. Morris, X. Qiao, D. Zhao, T. Salim, B. Chen, E. E. M. Chia and Y. M. Lam, *J. Mater. Chem. C*, 2018, **6**, 10301–10307.

8.   T. Hu, M. D. Smith, E. R. Dohner, M. J. Sher, X. Wu, M. T. Trinh, A. Fisher, J. Corbett, X. Y. Zhu, H. I. Karunadasa and A. M. Lindenberg, *J. Phys. Chem. Lett.*, 2016, **7**, 2258–2263.

9.   A. Yangui, D. Garrot, J. S. Lauret, A. Lusson, G. Bouchez, E. Deleporte, S. Pillet, E. E. Bendeif, M. Castro, S. Triki, Y. Abid and K. Boukheddaden, *J.Phys. Chem. C*, 2015, **119**, 23638–23647.

10. X. Wang, W. Meng, W. Liao, J. Wang, R. G. Xiong and Y. Yan, *J. Phys. Chem. Lett.*, 2019, **10**, 501–506.

11. M. D. Smith, A. Jaffe, E. R. Dohner, A. M. Lindenberg and H. I. Karunadasa, *Chem. Sci.*, 2017, **8**, 4497–4504.

12. Y. Y. Li, C. K. Lin, G. L. Zheng, Z. Y. Cheng, H. You, W. D. Wang, and J. Lin, *Chem. Mater.*, 2006, **18**, 3463–3469.

13. Y. Li, G. Zheng and J. Lin, *Eur. J. Inorg. Chem.*, 2008, **2008**, 1689–1692.

14. E. R. Dohner, E. T. Hoke and H. I. Karunadasa, *J. Am. Chem. Soc.*, 2014, **136**, 1718–1721.

15. E. R. Dohner, A. Jaffe, L. R. Bradshaw and H. I. Karunadasa, *J. Am. Chem. Soc.*, 2014, **136**, 13154–13157.

16. L. Mao, Y. Wu, C. C. Stoumpos, M. R. Wasielewski and M. G. Kanatzidis, *J. Am. Chem. Soc.*, 2017, **139**, 5210–5215.

17. L. Mao, P. Guo, M. Kepenekian, I. Hadar, C. Katan, J. Even, R. D. Schaller, C. C. Stoumpos and M. G. Kanatzidis, *J. Am. Chem. Soc.*, 2018, **140**, 13078–13088.

18. I. Neogi, A. Bruno, D. Bahulayan, T. W. Goh, B. Ghosh, R. Ganguly, D. Cortecchia, T. C. Sum, C. Soci, N. Mathews and S. G. Mhaisalkar, *ChemSusChem*, 2017, **10**, 3765–3772.

19. M. P. Hautzinger, J. Dai, Y. Ji, Y. Fu, J. Chen, I. A. Guzei, J. C. Wright, Y. Li and S. Jin, *Inorg. Chem.*, 2017, **56**, 14991–14998.

20. X. Li, P. Guo, M. Kepenekian, I. Hadar, C. Katan, J. Even, C. C. Stoumpos, R. D. Schaller and M. G. Kanatzidis, *Chem. Mater.*, 2019, **31**, 3582–3590.

21. B. Febriansyah, T. M. Koh, R. A. John, R. Ganguly, Y. Li, A. Bruno, S. G. Mhaisalkar and J. England, *Chem. Mater.*, 2018, **30**, 5827–5830.

22. B. Febriansyah, T. M. Koh, Y. Lekina, N. F. Jamaludin, A. Bruno, R. Ganguly, Z. X. Shen, S. G. Mhaisalkar and J. England, *Chem. Mater.*, 2019, **31**, 890–898.

23. K. Robinson, G. V. Gibbs, and P. H. Ribbe, *Science* **1971**, *172*, 567–570.

24. D. Cortecchia, S. Neutzner, A. R. Srimath Kandada, E. Mosconi, D. Meggiolaro, F. De Angelis, C. Soci and A. Petrozza, *J. Am. Chem. Soc.*, 2016, **139**, 39–42.

25. K. Pradeesh, K. Nageswara Rao and G. Vijaya Prakash, *J. App. Phys.*, 2013, **113**.

26. Y. Takahashi, R. Obara, K. Nakagawa, M. Nakano, J-Y. Tokita, and T. Inabe, *Chem. Mater.* 2007, **19**, 6312–6316.

27. Z. Yuan, C. Zhou, Y. Tian, Y. Shu, J. Messier, J. C. Wang, L. J. van de Burgt, K. Kountouriotis, Y. Xin, E. Holt, K. Schanze, R. Clark, T. Siegrist and B. Ma, *Nature Commun.*, 2017, **8**.

28. C. Zhou, H. Lin, Y. Tian, Z. Yuan, R. Clark, B. Chen, L. J. van de Burgt, J. C. Wang, Y. Zhou, K. Hanson, Q. J. Meisner, J. Neu, T. Besara, T. Siegrist, E. Lambers, P. Djurovich and B. Ma, *Chem. Sci.*, 2018, **9**, 586–593.

29. C. Zhou, H. Lin, H. Shi, Y. Tian, C. Pak, M. Shatruk, Y. Zhou, P. Djurovich, M.-H. Du and B. Ma, *Angew. Chem. Int. Ed.*, 2018, **57**, 1021–1024.